

1 The impact of acute temperature stress on hemocytes of invasive
2 and native mussels (*Mytilus galloprovincialis* and *M.*
3 *californianus*): DNA damage, membrane integrity, apoptosis and
4 signaling pathways

5
6 Cui-Luan Yao* and George N. Somero

7
8 Hopkins Marine Station, Department of Biology, Stanford University, Pacific Grove, CA 93950
9 USA

10 *Current address: Fisheries College, Jimei University, Xiamen, 361021, People's Republic of
11 China

12 *Author for correspondence (e-mail: cuiluanyao@yahoo.com)

13 **SUMMARY**

14 We investigated effects of acute heat- and cold stress on cell viability, lysosome membrane
15 stability, double- and single-stranded DNA breakage, and signaling mechanisms involved in
16 cellular homeostasis and apoptosis in hemocytes of native and invasive mussels, *Mytilus*
17 *californianus* and *M. galloprovincialis*, respectively. Both heat stress (28°C, 32°C) and cold stress
18 (2°C, 6°C) led to significant double- and single-stranded breaks in DNA. The types and extents of
19 DNA damage were temperature- and time-dependent, as was caspase-3 activation, an indicator of
20 apoptosis, which may occur in response to DNA damage. Hemocyte viability and lysosomal
21 membrane stability decreased significantly under heat stress. Western blot analyses of hemocyte
22 extracts with antibodies for proteins associated with cell signaling and stress responses [including
23 members of the phospho-specific Mitogen Activated Protein Kinase (MAPK) family (c-JUN
24 NH(2)-terminal kinase (JNK) and p38-MAPK) and apoptosis executor caspase-3] revealed that
25 heat- and cold stress induced a time-dependent activation of JNK, p38-MAPK and caspase-3 and
26 that these signaling and stress responses differed between species. Thermal limits for activation of
27 cell signaling processes linked to repair of stress-induced damage may help determine cellular
28 thermal tolerance limits. Our results show similarities in responses to cold- and heat stress and

29 suggest causal linkages between levels of DNA damage at both extremes of temperature and
30 downstream regulatory responses, including induction of apoptosis. Compared to *M. californianus*,
31 *M. galloprovincialis* might have a wider temperature tolerance due to a lower amount of single-
32 and double-stranded DNA damage, faster signaling activation and transduction, and stronger
33 repair ability against temperature stress.

34

35 Key words: apoptosis, cell signaling, DNA damage, hemocyte, *M. galloprovincialis*, *Mytilus*
36 *californianus*,

37 Running title: Thermal responses of *Mytilus* hemocytes

38

39

INTRODUCTION

40

41

42

43

44

45

46

47

48

49

50

51

52

53

54

55

56

57

58

59

60

61

62

63

64

65

66

Rocky intertidal ecosystems are commonly dominated by sessile species like mussels that encounter wide variation in abiotic conditions due to alternating periods of emersion and immersion during the tidal cycle and changes in air and water temperature due to season and latitude. Thermal stress has been shown to have pronounced influences on biogeographic and local-scale distribution patterns of many sessile species, including mussels of the genus *Mytilus* (Braby and Somero, 2006a; Jones et al., 2009, 2010). These temperature-correlated distribution patterns may be governed in large measure by the abilities of the species to cope with cellular-level damage induced by non-optimal temperatures. The emerging picture of the responses of mussels to heat stress is that rapid changes in the activities of signaling proteins, which often are a result of post-translational modifications of existing proteins (Evans and Somero, 2010) initiate diverse changes in cellular activity that function to restore cellular homeostasis. Several recent studies of congeners of *Mytilus* have shown that high temperature stress also induces changes in gene and protein expression that are indicative of damage to cellular structures and attempts by the cell to either repair this damage or, if this is not possible, to remove damaged proteins or cells from the tissue (Lockwood et al., 2010; Tomanek and Zuzow, 2010; Fields et al., 2012).

To extend the analysis of mechanisms used by congeners of *Mytilus* to cope with thermal stress and to further compare differences in stress responses between differently adapted congeners, we conducted studies that took advantage of the utility of hemocytes as an experimental system and that included a focus on cold stress as well as heat stress. Most previous studies of thermal stress in *Mytilus* have only examined effects of exposure to high temperature and have used tissues, typically gill or mantle, that contain a variety of types of cells. The work reported below exploited hemocytes, free cells in the extracellular fluids that perform a variety of functions, including immune defense, wound and shell repair, digestion, excretion, as well as transport of oxygen, nutrients and metabolites (Cheng et al., 1981; Cajaraville and Pal, 1995). Generally, there are two main populations of hemocytes, granulocytes and hyalinocytes, in mussels (Cajaraville and Pal, 1995; Carballal et al., 1997). Hemocytes afford the experimental

67 advantage of providing a tractable study system that is relatively well-defined in terms of cell type
68 and where such processes as loss of membrane integrity and damage to nuclear DNA can be more
69 readily examined with a variety of microscopic and biochemical and molecular techniques than in
70 the case of complex tissues.

71 In the studies described below, we used hemocytes from two congeners of *Mytilus*, the
72 ribbed mussel, *M. californianus*, a species native to the West Coast of North America, and the blue
73 mussel *M. galloprovincialis*, an invasive species from the Mediterranean Sea that entered coastal
74 California waters in the mid-20th century and has subsequently replaced the native blue mussel, *M.*
75 *trossulus*, over the southern portion of its previous biogeographic range (Geller, 1999; Braby and
76 Somero, 2006a, b; Schneider, 2008; Hilbish et al., 2010). A number of comparative studies of
77 these three congeners of *Mytilus* have shown *M. galloprovincialis* to be more heat tolerant than the
78 native blue mussel, and it has been conjectured that the further northward spread of the invader
79 may be facilitated by climate change (Braby and Somero, 2006a, b; Lockwood and Somero, 2011;
80 Fields et al., 2012). However, the effects of extreme low temperatures on congeners of *Mytilus*
81 have received little attention, so the potential for winter conditions to influence biogeographic
82 distributions remains largely unexplored. We thus used the hemocyte study system to examine the
83 effects of both heat- and cold-stress on cellular status.

84 In our experiments we sought to characterize in hemocytes the multi-level response that is
85 made in reaction to cellular damage, e.g., DNA breakage, from thermal stress, beginning with
86 stress signal transduction systems and terminating with programmed cell death in cases where
87 stress-induced damage cannot be repaired. The initial response to cellular stress commonly
88 involves rapid activation of various signal transduction pathways that lead to either restoration of
89 cellular homeostasis or, if this cannot be achieved, to cellular death (Kültz, 1995). p38
90 mitogen-activated protein kinases (MAPK), c-Jun N-terminal kinase (JNK, also called
91 stress-activated protein kinase, SAPK) and extracellular signal-regulated kinase (ERK) constitute
92 the family of MAPKs that commonly play key roles in the stress response. Among these systems,
93 the p38-MAPK and JNK pathways are mainly activated by environmental stress or cytokines
94 (Cowan and Storey, 2003). It was demonstrated that p38-MAPK and JNK activity showed a close
95 relationship with blockage of apoptosis after thermal stress in mammalian cells lines (Brown and

96 Benchimol, 2006; Murai et al., 2010). Although much less is known about these responses in
97 non-model species, p38-MAPK and JNK activation were shown to be induced by thermal stress in
98 gill, mantle tissue or posterior adductor muscle of *M. galloprovincialis* or the bearded horse
99 mussel *Modiolus barbatus* (Kefaloyianni et al., 2005; Anestis et al., 2007; Anestis et al., 2008;
100 Gourgou et al., 2010).

101 Cellular damage from thermal stress at the molecular level has most commonly been
102 investigated in proteins. Less understood—but of pivotal importance to the integrity of the
103 genome—is the role of temperature-induced damage to DNA. Many previous studies have shown
104 that DNA damage is induced by various environmental chemical stressors including genotoxic
105 substances, heavy metals, and organic contaminants (Micic et al., 2002; Klobučar et al., 2008;
106 Wepener et al., 2008). However, relatively little is known about effects of thermal stress on the
107 integrity of DNA. In *M. galloprovincialis* DNA damage was detected in mantle and gill tissue
108 following heat stress (Kefaloyianni et al., 2005), but the effects of both heat- and cold stress on
109 different types of DNA damage remain largely unknown. DNA single-stranded breakage (SSB) is
110 the most frequent type of DNA damage in stressed cells; SSBs are usually repaired correctly and
111 their effects on cellular survival or mutagenesis are relatively low (Wallace, 1994). However,
112 DNA double-stranded breakage (DSB) is far more threatening to cellular and genomic integrity
113 and may lead to cellular death through induction of apoptosis (Ori et al., 2005). When cellular
114 damage from stress crosses a certain threshold, notably in the case of severe damage to DNA that
115 cannot be adequately repaired, apoptosis may be initiated. Caspase-3, well-known as the
116 executioner caspase, plays a crucial role in apoptotic destruction of cells (Earnshaw et al., 1999;
117 Lakhani et al., 2006). Previous studies showed that caspase-3 transcripts increased after heat stress
118 in gill tissue (Lockwood et al., 2010) and heavy metal ion stress in mantle tissue (Kefaloyianni et
119 al., 2005) of *M. galloprovincialis*.

120 Membrane systems are another critical site of damage from stress (Hochachka and Somero,
121 2002). Damage to lysosomes is one example of this type of stress-induced lesion. Lysosomes are
122 found within the semi-granular and granular hemocytes of many marine invertebrates and are
123 released by a process of degranulation of hemocytes after environmental stresses (Hauton et al.,
124 1998; Camus et al., 2000). Once in the cytoplasm, the proteolytic enzymes that exist in lysosomes

125 are released and the hemocytes are lysed (Yao et al., 2008). Lysosomal neutral red retention (NRR)
126 time has proven to be a sensitive indicator of membrane integrity of hemocytes of blue mussels
127 and shrimp (Lowe et al., 1995; Camus et al., 2000; Yao et al., 2008). It was demonstrated that
128 lysosome stability and membrane integrity of hemocytes have a close relationship with animal
129 health status (Lowe et al., 1995; Yao et al., 2008). Furthermore, stress from low temperature also
130 can reduce NRR time; this effect was observed in cold-stressed *M. galloprovincialis* (Hauton, et
131 al., 1998; Camus et al., 2000). A recent study of thermal acclimation in the mussel *Modiolus*
132 *barbatus* found decreases in NRR retention time during prolonged acclimation at high
133 temperatures (28° and 30°C) (Dimitriadis et al., 2012).

134 In the present study we used hemocytes from two congeners of *Mytilus* to compare the
135 effects of acute heat- and cold stress on double- and single-stranded DNA breakage, lysosome
136 membrane stability, p38-MAPK and JNK phosphorylation and caspase-3 activation. Our results
137 indicate that DNA damage, stress-related signal transduction, and apoptosis play critical roles in
138 responses to stress from low and high temperatures by mussel hemocytes and interspecific
139 differences in these responses may influence the thermal optima and thus the distribution ranges of
140 the native and invasive congeners.

141

142 MATERIALS AND METHODS

143

Reagents

144 All chemicals were purchased from Sigma Chemical Co. (St. Louis, MO) and were of the
145 highest grade available. The enhanced chemiluminescence (ECL) kit was from GE Healthcare
146 (Uppsala, Sweden); the BCA protein assay reagent was from Pierce (Rockford, IL); and PVDF
147 membranes were from Amersham (Piscataway, NJ). Antibodies specific for the phosphorylated
148 forms of p38-MAPK (#9211) and JNKs (#9251) were obtained from Cell Signaling Technology
149 (Beverly, MA). A rabbit monoclonal antibody specific for caspase-3 (#9665) that detects the
150 endogenous levels pro-caspase-3 and active-caspase-3 was also purchased from Cell Signaling
151 Technology. The anti-actin antibodies (#sc10731), HRP-conjugated anti-rabbit (#sc-2004) and
152 anti-mouse (#sc-2055) antibodies were from Santa Cruz Biotechnology, Inc. (Santa Cruz, CA).
153 Prestained molecular mass standards were obtained from Bio-Rad (Hercules, CA). XOMAT AR

154 film was from Eastman Kodak Company (New York, NY).

155

156

Animal collections

157 Adult specimens of *M. galloprovincialis* (Lamarck 1819) (55-70mm length) were collected
158 subtidally near Santa Barbara, CA (34°24' N, 119°41' W). Animals were shipped to Hopkins
159 Marine Station and were maintained for four weeks at 13°C at a salinity of 31 parts per thousand
160 in recirculating seawater tanks and fed a phytoplankton diet every day as described by Lockwood
161 et al. (2010). *Mytilus californianus* (Conrad 1837) (55-70 mm length) were collected from mussel
162 beds in the exposed rocky intertidal zone at Hopkins Marine Station, Pacific Grove, CA (36°37' N,
163 121°54' W) and were acclimated under the same conditions used for *M. galloprovincialis*.

164

165

Acute temperature stress

166 Following the acclimation period, four groups of 15 mussels of each species were acutely
167 transferred from the 13°C holding aquaria to tanks containing either cold (2°C and 6°C) or warm
168 (28°C and 32°C) seawater, to determine the effect of acute temperature change on survival.
169 Survival times were based on numbers of dead animals at 8 h and 12 h after onset of acute stress.
170 Based on survivorship at low temperatures, mussels of both species (5 individuals for each group)
171 were immediately transferred from 13°C to 2°C and 6°C seawater aquaria for subsequent studies
172 of cold stress. For studies of acute heat stress, *M. californianus* were acutely transferred from
173 13°C to 24°C, 28°C and 32°C. For the more heat-tolerant *M. galloprovincialis*, transfers were
174 from 13°C to 28°C and 32°C. The mussels were sampled at 0.5 h, 2 h and 8 h after exposure to
175 acute temperature stress. Mussels from the 13°C acclimation population were sampled as controls.
176 Five mussels were sampled from each of the three treatment or control groups at each time point.
177 Mortality during exposures was scored if mussels failed to close their shells after external
178 stimulation. Only mussels exhibiting shell closure were used in the hemocyte experiments.

179

180

Hemocyte preparation

181 Hemolymph (1.2 ml per mussel) was collected from the posterior adductor muscle with a
182 20-gauge needle and 2 ml disposable syringe and combined with 0.3 ml of anti-coagulant solution,

183 a modified Alsever's solution (27 mmol l⁻¹ sodium citrate, 115 mmol l⁻¹ glucose, 336 mmol l⁻¹
184 NaCl, 18 mmol l⁻¹ EDTA, pH 7.0) (Li et al., 2009). Hemolymph from 5 mussels was pooled and
185 mixed together. 600 microliters of this fresh hemolymph were used immediately to examine
186 trypan blue exclusion, DNA integrity (comet assays), and neutral red retention by lysosomes. The
187 rest of the hemocytes were collected by 5 min centrifugation at 1500 g, 4°C. Then, the hemocytes
188 were resuspended in 1 ml 50 mmol l⁻¹ PBS buffer (137 mmol l⁻¹ NaCl, 7.8 mmol l⁻¹
189 Na₂HPO₄•12H₂O, 2.7 mmol l⁻¹ KCl, 1.47 mmol l⁻¹ KH₂PO₄, pH 7.4), washed twice with this
190 buffer and collected by sedimentation. The pelleted hemocytes were then immediately frozen in
191 liquid nitrogen and stored at -80 °C until used. The hemocytes pooled from 5 mussels at each time
192 point were mixed as one sample; three such pooled samples were generated. Thus, a total of 15
193 animals were used at a time-point (n=3 measurements per pooled sample).

194

195 **DNA damage assay**

196 Double-stranded and single-stranded DNA breakage were assessed using alkaline and
197 neutral single-cell gel electrophoresis (comet) assays, respectively. Double-stranded DNA damage
198 was detected according to a protocol described by Singh et al. (Singh et al., 1988) with slight
199 modifications (Klobučar et al., 2008). Briefly, 75 µl of hemolymph mixed with 0.8% low melting
200 point (LMP) agarose were placed on a 0.75% agarose pre-coated microscope slide. After
201 solidifying for 5 min at 4°C in the dark, a third layer of 0.5% LMP agarose was added and left to
202 solidify as described. The cells were lysed in freshly made lysing solution (2.5 mol l⁻¹ NaCl, 100
203 mmol l⁻¹ Na₂EDTA, 10 mmol l⁻¹ Tris base, 10% DMSO, 1% Triton X-100, pH 10) for 1 h at 4°C
204 in the dark. Then, the slides were rinsed with cold alkaline electrophoresis solution for 5 min (300
205 mmol l⁻¹ NaOH, 1 mmol l⁻¹ EDTA, pH >13) and then placed on a horizontal gel box and covered
206 with the same buffer for 20 min. The slides then were subjected to electrophoresis for 20 min at 25
207 V, 4°C.

208 Single-stranded DNA damage was assessed using the neutral comet assay. The procedure
209 was conducted similarly to the alkaline assay but with the following lysis buffer: 2.5 mol l⁻¹
210 NaCl, 100 mmol l⁻¹ EDTA, 10 mmol l⁻¹ Tris-HCl, 1% *N*-lauroylsarcosine, 0.5% Triton X-100,
211 10% dimethylsulphoxide (DMSO) at pH 9.5. After 1 h of lysis the slides were washed three times

212 with electrophoresis buffer (300 mmol l⁻¹ sodium acetate, 100 mmol l⁻¹ Tris-HCl, pH 8.3) and left
213 in a fresh electrophoresis solution for 1 h. Then the slides were electrophoresed for 1 h at 14V (0.5
214 V/cm, 11–12 mA), 4°C.

215 After alkaline electrophoresis the slides were neutralized in cold neutralization buffer (0.4
216 mol l⁻¹ Tris/HCl, pH 7.5), 2×5 min. The slides were stored in the dark at room temperature and
217 stained with a fluorescent dye (SYBR green). The slides were stored overnight at 4°C in light-tight
218 humidified boxes and analyses were performed the following day. For each slide, pictures of 100
219 randomly selected hemocytes (pooled from 5 individuals) were captured at 400 X magnification
220 using a fluorescence microscope (Olympus). DNA damage was assessed using CASP version
221 1.2.2 (Comet Assay Software Project, <http://casplab.com/>). Triplicate analyses were done for each
222 group. Estimates of the extent of DNA strand breakage are expressed as the percent of DNA found
223 in the tail of the comet (%DNAT). %DNAT = (100 x DNAT)/(DNAH+DNAT). Here, DNAH
224 (DNA head) is the sum of intensities of all points within the head of the comet and DNAT is sum
225 of intensities of all points of the tail (Końca et al., 2003) (Fig. 1).

226

227

Cell viability

228 Cell viability was assessed by the trypan blue (Sigma, T8154) exclusion test, using a
229 hemocytometer to manually count viable and nonviable cells. Briefly, 10 µl of a 0.4% solution of
230 the dye were added to 50 µl of hemocyte suspension. The numbers of stained (blue = nonviable)
231 and unstained (transparent = viable) hemocytes were counted using an optical microscope. For
232 each sample (pooled hemocytes from 5 mussels), a minimum of 200 cells were counted in a total
233 of 10 microscopic fields for each of 3 replicate preparations. Thus, a total of 9 slides representing
234 3 samples from 15 animals at each time point were used for analysis.

235

236

Lysosomal Stability

237 The stability of hemocyte lysosomes was determined using a neutral red retention protocol
238 (Lowe and Pipe, 1994; Lowe et al., 1995). Briefly, the neutral red stock solution was made by
239 dissolving 20 mg of dye in 1 ml of DMSO. The working solution was prepared by diluting 5 µl of
240 stock solution in 2.5 mmol l⁻¹ of PBS. Approximately 50µl of hemocyte suspension were placed

241 carefully on each slide. Slides then were placed in a light-proof, controlled humidity chamber for
242 20 min, after which the excess solution was carefully removed and 20 μ l of freshly made neutral
243 red working solution were added. The slides were incubated in the controlled humidity chamber
244 for an additional 20 min and then were observed under an optical microscope at 400 X
245 magnification. Tests were terminated when dye loss was evident in approximately 50% of the
246 hemocytes.

247

248

Protein extractions

249 Based on initial morphological studies of hemocyte lysis, we determined temperatures of
250 exposure and collection of hemocytes that would ensure capture of largely viable populations from
251 both species. Because most hemocytes of *M. californianus* were lysed at 32°C, hemocytes of this
252 species were collected at 2°C and 28°C. Hemocytes of *M. galloprovincialis* were collected at 2°C,
253 28°C and 32°C. Hemocytes pellets (see Hemocyte Preparation) were added to 1 volume lysis
254 buffer (50 mmol l^{-1} Tris-HCl, pH 7.8, 250 mmol l^{-1} sucrose, 1% SDS, 0.1% NP-40) containing
255 Complete Mini proteinase inhibitor Mix (Roche Applied Science, Indianapolis IN) (1 tablet / 10
256 ml). The proteins were extracted by submitting hemocytes to three 20s bursts of sonication
257 (Branson sonicator, setting 5) in an ice-cold water bath. The samples were centrifuged at 12,000 x
258 g for 10min at 4°C and the supernatants were collected. Total protein concentrations were
259 determined using the BCA assay (Pierce, Rockford, IL, USA).

260

261

SDS-PAGE and western blotting

262 Thirty ng of supernatant protein were boiled with 0.33 volumes of SDS-PAGE sample
263 buffer [0.33 mol l^{-1} Tris/HCl, pH 6.8, 10% (w/v) SDS, 13% (v/v) glycerol, 20% (v/v)
264 2-mercaptoethanol, 0.2% (w/v) bromophenol blue] for 3 min. The samples were loaded onto 12%
265 (w/v) acrylamide, 0.33% (w/v) bisacrylamide Tris-HCl polyacrylamide gels. Electrophoretically
266 separated proteins were wet transferred to PVDF membranes for 2 h at 4°C. Resulting blots were
267 blocked for 1 h in 5% blocking grade non-fat dried milk dissolved in Tris buffered saline (250
268 mmol l^{-1} Tris-HCl pH 7.5, 1.5 mol l^{-1} NaCl) containing 0.1% Tween-20 (TBST), washed 2 X 5
269 min in TBST, and incubated with the appropriate primary antibody according to the

270 manufacturer's instructions.

271 Antibodies to detect phosphorylation on p38-MAPK (Thr-180/Tyr-182) and JNK/SAPK
272 (Thr-183/Tyr-185), caspase-3 and actin were diluted to 1: 1000 in the same buffer. Following 3 X
273 5 min washes in TBST, blots were incubated with the corresponding secondary antibody (goat
274 anti-rabbit (sc-2004) or goat anti-mouse (sc-2055) (Santa Cruz Biotechnology, Inc., Santa Cruz
275 CA). The secondary antibody was diluted 1:3000 in 5% BSA in TBST and incubated for 60 min at
276 room temperature with gentle agitation. Following 6 X 5 min washes in TBST, blots were treated
277 with enhanced chemiluminescent reagent (Amersham, Piscataway, NJ) for 2 min. Finally, blots
278 were exposed to Kodak X-Omat AR film and developed. The bands were quantified by laser
279 scanning densitometry. Equal protein loading was verified by probing identical samples with an
280 anti-actin antibody (whole extracts). Densitometric analyses were performed using ImageJ
281 software (<http://rsb.info.nih.gov/ij/>). For the phospho-JNK/SAPK antibody, which detected two
282 bands at 46 and 54 kDa, and for the caspase-3 antibody, which detected the endogenous levels of
283 full-length (35 kDa) and large active fragments (17/19 kDa) of caspase-3, density was calculated
284 as the intensity of the corresponding band. Blots and results shown are representative of three
285 independent experiments. Results are means \pm s.e. for three independent experiments.

286

287

Statistical analysis

288 The data were analyzed by two-way analysis of variance (two-way ANOVA) using SPSS
289 13.0 for Windows (SPSS Inc.). Statistical significance was determined by two-way ANOVA with
290 stress time and temperature as factors. A least significant difference (LSD) post hoc test ($p < 0.05$)
291 was used to resolve statistically significant differences between stress temperature and stress time.
292 Asterisks denote statistically significant differences between experimental treatments (high- and
293 low temperature stress for varying times) and the control (13°C specimens).

294

295

RESULTS

296

Survival at low and high temperatures

297 The effects of acute cold- and heat stress on the survival of *M. californianus* and *M.*
298 *galloprovincialis* were assessed by acutely exposing mussels to 2°C, 6°C, 24°C, 28°C and 32°C

299 and monitoring survival. For *M. californianus*, 73.3% and 20% of specimens exposed to 32°C and
300 28°C, respectively, died within 12 h (data not shown). 13.3% of *M. californianus* died within 8 h
301 after exposure at 32°, but no mortality was found at 8 h after stress at 28°C. For *M.*
302 *galloprovincialis* no deaths were observed after exposure at 28°C or 32°C for 8 h. For cold stress,
303 no deaths were observed for either species following exposure to 2°C for 8 h. Thus, our results
304 indicate interspecific differences in tolerance of high temperatures but similar tolerance of low
305 temperatures.

306

307

DNA damage

308 DNA damage by environmental stress is frequently assessed by the comet assay (Singh et
309 al., 1988). Cells with damaged DNA show increased migration of DNA fragments from the
310 nucleus (“head” of comet) into the trailing (“tail”) region of the comet; the length of the tail
311 indicates the distribution of fragment sizes and the area of the tail provides a measure of total
312 amount of DNA strand breakage. The most frequently used parameter for the determination of
313 total DNA damage is the percentage of DNA in the comet’s tail (Ashby et al., 1995). A
314 representative image of the comet geometry observed in thermally stressed mussel hemocytes is
315 shown in Fig.1.

316 Levels of single-stranded DNA damage in hemocytes are shown in Fig. 2. In hemocytes of
317 *M. californianus* at the control temperature (13°C), DNA with single-stranded breakage (SSB)
318 represented about 30% of total DNA (Fig. 2A). SSBs increased significantly (approximately
319 doubling) after 8 h stress at 2°C and 6°C ($p<0.05$). Significant increases of SSBs occurred more
320 rapidly under heat stress and were detected after 0.5 and 2 h exposure at 32°C ($p<0.05$).
321 However, after 8 h at 32°C, the level of SSBs did not differ from control values.

322 The levels of SSBs in *M. galloprovincialis* hemocytes following different temperature
323 stresses are shown in Fig. 2B. In control hemocytes, a lower fraction of the DNA was found in the
324 tail of comet, approximately 5%, than in the case of *M. californianus*. However, as in the latter
325 species, SSBs in hemocytes of *M. galloprovincialis* increased under both low- and high
326 temperature stress, with the greatest tail DNA value, 50.3%, found after 8 h exposure at 32°C
327 ($p<0.05$).

328 The extent of double-stranded DNA breakage (DSB) in hemocytes under control
329 conditions (13°C) (Fig. 3) was much less than the extent of SSB (Fig. 2). Distinct interspecific
330 differences were noted, with damage in hemocytes of *M. californianus* being greater than in
331 hemocytes of *M. galloprovincialis* at the corresponding time and stress temperature (Fig. 3). In *M.*
332 *californianus* hemocytes, DSBs increased gradually from the beginning of thermal stress and
333 reached a peak value after 8 h exposure at 2°C, 6°C, 24°C and 28°C (Fig. 3A). At 32°C, however,
334 DSBs increased sharply after 0.5 h exposure and the high value was maintained to 8 h, with
335 approximately 95% of the DNA occurring in the tail region of the comet. In *M. galloprovincialis*
336 hemocytes, DSBs showed a gradual increase after cold- or heat stress and did not reach values as
337 high as those found for its congener (note the different ordinate ranges in Fig.3A and B). The most
338 serious damage appeared at 8 h after cold- and heat stresses ($p<0.05$), with the peak value of
339 approximate 50% tail DNA at 8 h after stress at 32°C (Fig. 3B).

340 In summary, hemocytes of the two congeners exhibited large differences in SSBs and
341 DSBs under most conditions. SSB levels were generally higher in *M. californianus* hemocytes,
342 including under control conditions. DSB levels were temperature- and time-dependent in both
343 species after cold and heat stress. As in the case of SSBs, higher levels of DSBs were found in *M.*
344 *californianus* hemocytes under most experimental conditions. These data suggest that thermal
345 stress has significant effects on the integrity of DNA and that this stress varies between congeners.
346 Thus, in the case of DSBs, *M. californianus* hemocytes attained extremely high levels of DSBs at
347 elevated temperature (32°C), levels that were approximately twice those observed in *M.*
348 *galloprovincialis*.

349

350 **Stress response: p38-MAPK and JNK/SAPK activation**

351 For *M. californianus*, p38 phosphorylation level increased significantly after 2 h of cold
352 stress at 2°C, with the highest expression reaching 1.8 times that of the control group ($p<0.05$)
353 (Fig. 4A). The phosphorylation level then gradually decreased, but a moderately high expression
354 of phospho-p38 was maintained to 8 h, although this level was not significantly different from the
355 control. Exposure to 28°C did not lead to significant changes in phospho-p38 levels. For *M.*
356 *galloprovincialis*, phospho-p38 increased significantly from 0.5 h to 2 h ($p<0.05$) after cold stress

357 at 2°C, and then returned to the control level at 8 h (Fig. 4B). After high temperature stress at
358 28°C, phospho-p38 increased gradually with exposure up to 8 h, reaching a peak value 4 times
359 that of the control group ($p<0.05$). At 32°C, phospho-p38 increased significantly at 0.5 h ($p<0.05$),
360 returned to control levels at 2 h, and then increased again from 2 to 8 h of stress ($p<0.05$) (Fig.
361 4B).

362 Expression profiles of phospho-JNK (Thr-183/Tyr-185) (46 kDa bands for phospho-JNK1,
363 54 kDa bands for phospho-JNK2/3) at different temperature stresses are shown in Fig. 4C-F. In *M.*
364 *californianus*, the expression level of phospho-JNK1 (46 kDa) decreased sharply at 0.5 h after
365 cold stress at 2°C ($p<0.05$), however, it returned to control levels between 2 to 8 h. After heat
366 stress at 28°C, phospho-JNK1 showed a significant decrease at 2 h ($p<0.05$), and then recovered to
367 that of the control level at 8 h (Fig. 4C). In *M. galloprovincialis*, phospho-JNK1 (46 kDa) showed
368 a gradual increase after cold stress at 2°C, with the highest level appearing at 8 h ($p<0.05$) (Fig.
369 4D). After heat stress, phospho-JNK1 (46 kDa) increased gradually from 0.5 to 8 h at 28°C
370 ($p<0.05$), reaching a peak value of 3.2 times the control level at 8 h after heat stress at 28°C. The
371 phospho-JNK1 (46 kDa) level showed a significant increase from 0.5 and 8 h at 32°C ($p<0.05$)
372 (Fig. 4D). Phospho-JNK2/3 in *M. californianus* (54 kDa) also dropped sharply at 0.5 h under 2°C
373 exposure ($p<0.05$); then it recovered moderately at 2 h but decreased again at 8 h ($p<0.05$).
374 Phospho-JNK2/3 (54 kDa) showed similar changes to JNK1 after heat stress at 28°C (Fig. 4E). In
375 *M. galloprovincialis*, Phospho-JNK2/3 (54 kDa) also increased significantly at 0.5 and 8 h
376 ($p<0.05$) with the peak value 5.3 times that of the control group ($p<0.05$) at 8 h after 2°C stress
377 (Fig. 4F). After heat stress at 28°C, phospho-JNK2/3 (54 kDa) level increased sharply at 0.5 h
378 ($p<0.05$) and then gradually returned to the control level at 8 h. A similar change of
379 phospho-JNK2/3 was found after heat stress at 32°C; phosphorylation level of JNK2/3 increased
380 significantly at 0.5 h ($p<0.05$) and then decreased gradually from 0.5 to 8 h after stress at 32°C,
381 with the significant decrease expression appeared at 8 h ($p<0.05$) (Fig. 4F).

382 Overall, our results showed that the phosphorylation level of p38 and JNKs in *M.*
383 *galloprovincialis* hemocytes after cold and heat stress increased faster and reached high levels
384 than in the case of *M. californianus*.

385

Apoptosis initiation: caspase-3 activation

386

387 The caspase-mediated apoptotic death induced by diverse stressful conditions is well
388 characterized in mammalian cell types (for a review, see Jiang and Wang, 2004). Expression
389 profiles of pro- and active-caspase-3 in hemocytes after cold- and heat stress are shown in Fig.5.
390 In *M. californianus*, pro-caspase-3 expression increased significantly at 0.5 h after cold stress at
391 2°C, and then decreased gradually even though a significantly higher level of pro-caspase-3
392 expression was maintained out to 8 h of exposure ($p<0.05$). At 28°C, pro-caspase-3 expression
393 showed a similar change with that of cold stress ($p<0.05$) (Fig. 5A). In *M. galloprovincialis*,
394 pro-caspase-3 expression showed significant increase at 0.5 h after cold stress at 2°C, after which
395 it decreased gradually and returned to the control level at 8 h (Fig. 5B). At 28°C, pro-caspase-3
396 was up-regulated significantly from 0.5 h to 8 h after stress, with the peak value at 8 h of 3.15
397 times that of the control group. Pro-caspase-3 also increased significantly from 0.5 to 8 h after
398 heat stress at 32°C ($p<0.05$), but the highest level was lower than the group under 28°C stress (Fig.
399 5B).

400 Active-caspase-3 expression in *M. californianus* increased sharply at 0.5 h ($p<0.05$) after
401 cold stress at 2°C; subsequently, it decreased although significantly higher expression lasted to 8 h
402 after stress ($p<0.05$) (Fig. 5C). At 28°C, active-caspase-3 expression levels showed a gradual
403 increase from 0.5 to 8 h after stress, with significantly higher expression levels occurring at 2 and
404 8 h ($p<0.05$) (Fig. 5C). In *M. galloprovincialis*, active-caspase-3 showed significant enhancement
405 at 0.5 h after cold stress at 2°C, but decreased gradually and returned to the control level at 8 h
406 (Fig. 5D). At 28°C active-caspase-3 expression level increased gradually from 0.5 h to 8 h
407 ($p<0.05$), with the peak value appearing at 8 h after stress. At 32°C, significantly higher
408 expression of active-caspase-3 was found at 0.5 and 2 h ($p<0.05$); expression returned to the
409 control level at 8 h of stress (Fig. 5D).

410 In summary, caspase-3 expression could be induced by both cold and heat stress in the two
411 species. However, the species differed in their responses in terms of total levels of the protein and
412 the time-courses of the response. For example, after exposure to 28°C the highest pro-caspase-3
413 level was detected at 0.5 h in *M. californianus* hemocytes whereas the greatest pro-caspase-3
414 expression in *M. galloprovincialis* was found at 8 h.

415

416

Temperature stress causes necrosis and lysis of hemocytes

417

418

419

420

421

422

423

424

425

Hemocyte viability was assessed using the trypan blue exclusion test. At the control temperature of 13°C, fewer than 5% of *M. californianus* hemocytes were non-viable (Fig. 6A). Cold- and heat stress led to significant increases in percentages of nonviable cells. The hemocytes of *M. californianus* were ~10% non-viable after 0.5 h of cold stress at 2°C, and the fraction of non-viable hemocytes increased to 27% at 2 h and 22.7 % at 8 h after stress at 2°C. At 6°C, the viability of hemocytes showed similar changes to those found with the 2°C stress group. At 24°C, percentage of non-viable hemocytes showed a gradual increase from 0.5 to 8 h. Under 32°C stress, the percentage of non-viable hemocyte gradually increased with time of stress, with a peak value of 40% at 8 h ($p<0.05$).

426

427

428

429

430

431

432

433

Hemocyte viability for *M. galloprovincialis* is shown in Fig. 6B. Under control (13°C) conditions, hemocyte viability was near 98% at all time points. After cold stress at 2°C, the non-viable hemocytes showed a gradual increase from 0.5 h to 8 h, with the highest value of 15.7 % non-viable hemocytes appearing at 8 h. There was no significant difference between cold stress at 2°C and at 6°C. After heat stress at 28°C, hemocyte non-viability showed a gradual increase from 0.5 h to 8 h. At 32°C, hemocyte viability showed a similar change to that seen in the specimens exposed to 28°C, with the greatest percentage of non-viable hemocytes reaching 34% ($p<0.05$).

434

435

436

437

438

439

440

441

Stability of lysosomal membranes in hemocytes was assessed using the neutral red retention assay (Fig. 7). Both cold- and heat stress reduced neutral red retention times (NRRT) significantly. In *M. californianus*, the NRRT was ~ 109 min at 13°C. After cold stress at 2°C, the NRRT decreased to 60 min at 0.5 h and continued decreasing from 0.5 to 8h, with the shortest NRRT of ~30 min at 8 h ($p<0.05$). The NRRT after cold stress at 6°C showed a similar pattern to that seen in the group under 2°C stress. Additionally, the NRRT decreased significantly after stress at 24°C, 28°C and 32°C. NRRT showed time- and temperature-dependent patterns, with the shortest NRRT of ~10 min at 8 h after heat stress at 32°C (Fig. 7A).

442

443

In *M. galloprovincialis*, the NRRT was >120 min in the control group (13°C). During exposure to 2°C NRRT showed a gradual decrease from 0.5 to 8 h; the shortest NRRT (~70 min)

444 occurred at 8 h. At 6°C, a similar pattern to that seen at 2°C was observed; however, the NRRT
445 was longer than that of the 2°C specimens at corresponding time points. After stress at 28°C,
446 NRRT was ~100 min at 0.5 h; it then decreased gradually and reached a minimal value of ~59 min
447 at 8 h. At 32°C, NRRT decreased sharply, with the smallest value of ~30 min occurring at 8 h of
448 stress exposure ($p<0.05$) (Fig. 7B).

449 Overall, although both species showed qualitatively similar responses to thermal stress in
450 viability and NRRT, the percentage of non-viable hemocytes typically was higher and the NRR
451 time generally was shorter in *M. californianus* than in *M. galloprovincialis* at the corresponding
452 temperature and time point. Differences after 2 hours of cold stress were especially marked
453 between species.

454

455 DISCUSSION

456

457 Whole organism thermal tolerance

458 After acute high temperature stress, *M. californianus* showed a much higher mortality
459 (73.3% at 32°C for 12 h) and a lower high temperature limit (28°C for 8 h) than *M.*
460 *galloprovincialis*, which survives at 32°C for 8 h. These findings agree with those of previous
461 studies that demonstrated that *M. galloprovincialis* is a warm-adapted species relative to its
462 congeners (Braby and Somero, 2006b; Fields et al., 2006; Lockwood and Somero, 2011; Fields et
463 al., 2012). *M. californianus* and *M. galloprovincialis* could survive for 8 h at 2°C, suggesting that
464 both species may be tolerant of cold extremes at least over short time intervals. However, their
465 mortality and tolerance ability after long term exposure need further study.

466

467

468 DNA damage

468 DNA is vulnerable to damage from a variety of toxic insults, including those that result
469 from normal metabolic activities, e.g., the production of reactive oxygen species, and from
470 physical and chemical environmental stressors. DNA damage due to combinations of
471 environmental factors and normal metabolic processes occurs at a high rate in human cells and
472 increases under environmental stress (Roberts et al., 2006; Prasad et al., 2011). Single base lesions

473 causing single-stranded breakage are the most common forms of DNA damage (Roberts et al.,
474 2006; Prasad et al., 2011). Although SSBs can generally be repaired, they are known to be the
475 initial signal for activating the SOS repair response in bacteria (Craig and Roberts, 1981) and to
476 act as the initial signal for DNA damage responses in eukaryotic cells (Li and Deshaies, 1993). A
477 number of studies have demonstrated that production of SSBs can influence the cell cycle and
478 induce cell death, indicating a broad potential role of single-stranded DNA in DNA damage
479 signaling.

480 The amounts of SSB and DSB in hemocytes from mussels subjected to heat- and cold
481 stresses varied between species and with temperature and time of exposure to stress. In the case of
482 SSBs, in hemocytes of *M. californianus* at the control temperature of 13°C, a typical seawater
483 temperature in Monterey Bay, approximately 30% of the total DNA was in the tail of the comet,
484 indicating a substantial number of SSBs even in the absence of thermal stress. In contrast, in
485 hemocytes of *M. galloprovincialis* only ~5-10% of the DNA reflected SSBs at 13°C (Fig. 2). Cold
486 stress (2°C and 6°C) led to increased SSB in both species, but a higher level of SSB again
487 occurred in *M. californianus*. Heat stress at 28°C and 32°C also increased levels of SSBs. Similar
488 amounts of SSBs were seen in the two congeners under heat stress.

489 Double-stranded breaks are thought to be the most serious form of DNA damage because
490 they can impede transcription, replication, and chromosome segregation (Nitiss, 1998). The
491 percentage of DSBs was low in hemocytes of both species at 13°C (Fig. 3). Cold stress and heat
492 stress both led to significant increases in DSBs, with *M. californianus* showing a higher level of
493 DSBs than its congener under all conditions of stress. Thus, at 32°C, 8 h of exposure led to
494 approximately 100% DSBs in hemocytes in *M. californianus*, whereas this stress exposure led to
495 only about 50% DSBs in *M. galloprovincialis*. The interspecific differences in DSBs under cold
496 and heat stress suggest a greater thermal tolerance range for DNA stability in *M. galloprovincialis*
497 relative to *M. californianus*. In accord with interspecific differences among congeners of *Mytilus*
498 in other physiological traits (Lockwood and Somero, 2011), the higher resistance of *M.*
499 *galloprovincialis* to thermally induced damage to DNA, notably in DSB levels, could be important
500 in conferring on this species its capacity to invade a variety of habitats.

501 The findings of significant and species-specific damage to DNA under cold- and heat

502 stress indicate that the role of damage to DNA under different environmental conditions merits
503 further study in the contexts of energetic costs for repair, for example in cases where severe DNA
504 damage leads to apoptosis, and potential compromise of the integrity of the genome.

505

506

Stress signaling proteins

507 Recently, studies have demonstrated that p38-MAPK and JNK play crucial roles in the
508 adaptive responses to thermal, osmotic, oxidative and heavy metal stresses in mussels
509 (Kefaloyianni et al., 2005; Gaitanaki et al., 2007; Evans and Somero, 2010; Gourgou et al., 2010).
510 For example, hyperthermia (30°C), hypothermia (4°C) and heavy metals induced a significant
511 activation of p38-MAPK in gill and mantle tissue of *M. galloprovincialis* (Kefaloyianni et al.,
512 2005). Significant p38-MAPK activation was detected in *M. galloprovincialis* mantle tissue after
513 oxidative and hypertonic stress (Gaitanaki et al., 2004), and in *M. galloprovincialis* and *Modiolus*
514 *barbatus* mantle tissue after high temperature stress (Anestis et al., 2007; Anestis et al., 2008).

515 Significant increase of phospho-p38-MAPK was detected in hemocytes of *M. californianus*
516 and *M. galloprovincialis* after cold stress at 2°C, suggesting that phosphorylation of p38-MAPK
517 played an important role in response to cold stress in both species. Gaitanaki and colleagues
518 (Gaitanaki et al., 2004) demonstrated that cold temperature stress (4°C) induced a moderate
519 phospho-p38-MAPK response in mantle tissue of *M. galloprovincialis*. Our results showed that
520 phospho-p38-MAPK level increased significantly in hemocytes of *M. galloprovincialis* at 28°C;
521 however, it did not show significant change in hemocytes of *M. californianus* under this condition.
522 Similarly, exposure to high temperature was found to cause a significant and sustained stimulation
523 of p38-MAPK phosphorylation in the gill tissue of *M. galloprovincialis* (Gourgou et al., 2010;
524 Kefaloyianni et al., 2005). Our results indicate that *M. californianus* might lose this component of
525 the cellular stress response at temperatures of 28°C and higher, whereas *M. galloprovincialis*
526 retains this ability. This cellular-level difference in thermal limits of signaling ability might be one
527 of the factors that contribute to the higher heat tolerance of *M. galloprovincialis* (Fig. 4B).

528 Evans and Somero (Evans and Somero, 2010) demonstrated that up-regulation of
529 phospho-JNK/SAPK increased significantly in gill of *M. galloprovincialis* after heat stress at 32°C
530 while it decreased significantly by 24°C in *M. californianus*. Gill tissue of *M. galloprovincialis*

531 (Gourgou et al., 2010) and mantle tissue and posterior adductor muscle of both *M.*
532 *galloprovincialis* and *M. barbatus* also showed activation of JNK at high temperature (Anestis et
533 al., 2007; Anestis et al., 2008), suggesting a common cellular stress response to heat stress in
534 different cell types of these two mussels. Results of the present study showed that both cold- and
535 heat stress induced a significant increase in JNK phosphorylation in hemocytes of *M.*
536 *galloprovincialis*, with the strongest expression at 28°C. However, compared with p38-MAPK,
537 JNK/SAPK activation was relatively moderate. In contrast, in *M. californianus* JNK
538 phosphorylation showed a significant decrease after cold stress at 2°C and heat stress at 28°C,
539 suggesting that a stronger response of phosphorylation of p38-MAPK and JNK to the low- and
540 high temperature stress existed in hemocytes of the invasive species *M. galloprovincialis*.

541 The different response of p38-MAPK and JNKs might be due to their different roles in
542 hemocytes in the face of temperature stress. Exposure of *M. galloprovincialis* to 30°C was found
543 to cause a significant and sustained stimulation of p38-MAPK phosphorylation while the
544 activation profile of JNKs was transient and relatively moderate in gill tissue (Gourgou et al., 2010;
545 Evans and Somero, 2010). It was demonstrated that the p38-MAPK phosphorylation was activated
546 more rapidly and strongly than that of JNKs in the isolated perfused heart of the frog *Rana*
547 *ridibunda* at 42°C (Gaitanaki et al., 2008), further indicating that p38 and JNKs might play
548 different roles in animals during temperature stress.

549 Because stress-induced kinases play a number of different roles, ranging from modulating
550 repair mechanisms to directing cells to apoptosis, and because they interact among themselves in
551 complex fashions to shape the overall responses of cells to stress, it is not possible to discern from
552 the present data how the species differ in the ultimate cellular responses governed by these
553 molecules. Thus, study needs to be extended to elucidate adequately the downstream
554 consequences of changes in the abundances and post-translational modification states of these
555 signaling proteins, e.g., whether or not apoptosis is triggered.

556

557 **Caspase-3 activation**

558 Caspase-3 is one of the key enzymes in apoptotic destruction of cells and is called the executioner
559 caspase (Earnshaw et al., 1999). Caspase-3 expression increased significantly in hemocytes of

560 both species after heat stress, suggesting that single- and double-stranded DNA damage could not
561 be adequately repaired in either species under these extremes of temperature (Fig. 5) and that
562 apoptosis may have been the end-result of this damage.

563 Note that in hemocytes of *M. galloprovincialis* exposed to 32°C, pro-caspase-3 and active
564 caspase-3 levels were lower than those measured in 28°C-exposed specimens (Fig. 5B,D). In a
565 study of transcriptional responses to heat stress, caspase-3 transcripts increased after heat stress in
566 gill tissue of *M. galloprovincialis* after exposure to 28°C, but decreased after exposure at 32°C
567 (Lockwood et al., 2010). The lower levels of caspase-3 mRNA and pro- and active-caspase-3
568 observed at 32°C likely reflect thermal disruption of caspase synthesis and post-translational
569 processing, not a reduced level of DNA damage at 32°C. In fact, DSB damage was higher at 32°C
570 than at 28°C (Fig. 3B). Thus, near 32°C, a key component of the regulatory network needed for
571 completing the cellular stress response may be disabled in this species. Thermal limits for essential
572 components of the cellular stress response may be instrumental in establishing whole organism
573 lethal temperature ranges.

574 At 2°C both species exhibited increased active-caspase-3 expression (Fig. 5), which reflected the
575 general pattern of DSB observed at low temperature (Fig. 3). Active caspase-3 levels remained
576 above control (13°C) levels in *M. californianus* out to 8 h of exposure to cold, but those of *M.*
577 *galloprovincialis* decreased to control values by 8 h. These interspecific differences may reflect
578 variations in levels of DNA damage and in DNA repair capacity, as discussed above.

579

580 **Hemocyte viability and lysosome integrity**

581 Hemocyte viability generally decreased with exposure time during low- and
582 high-temperature stress in both species (Fig. 6). The species responded similarly to exposure to
583 28°C and 32°C, but *M. galloprovincialis* was slightly less sensitive to heat stress. There was no
584 difference between the congeners in hemocyte viability during acute cold exposure.

585 Stability of lysosomal membranes as indexed by NRRT also decreased in a time-dependent
586 manner under cold- and heat stress (Fig. 7). NRRT generally reached lower values in *M.*
587 *californianus*, suggesting lower membrane stability in this species. Reductions in hemocyte
588 viability and NRRT appear to be generally useful indices of cellular stress. Previous studies also

589 have demonstrated that hemocyte viability and lysosome membrane stability decreased when the
590 animal suffered from environmental stress or pathogenic infection (Hauton et al., 1998; Camus et
591 al., 2000; Yao et al., 2008; Parolini et al., 2011).

592

593

Conclusions

594 The results of the present study demonstrate the utility of hemocytes as an experimental system
595 for examining a number of aspects of cellular thermal stress in marine mollusks and other taxa that
596 possess these types of cells. Stress from low- and high temperatures led to increased DNA damage
597 in hemocytes of *M. californianus* and *M. galloprovincialis*, notably in the case of DSBs. DNA
598 damage may be important per se, due to effects on genome integrity, as well as serving as a critical
599 factor in downstream initiation of apoptosis. The finding that stress from low temperatures (2°C
600 and 6°C) led to levels of DSB similar to and, at times, higher than the DSB levels found under
601 heat (28°C) stress suggests that more extensive analysis of cold stress—which commonly has
602 received less attention than heat stress—is warranted. This conclusion is supported as well by the
603 findings that cellular viability and lysosomal membrane integrity are also compromised at low, as
604 well as at high temperatures. Likewise, and in concert with the findings of DNA damage at low
605 and high extremes of temperature, the finding that caspase-3 levels increased under exposure to
606 low as well as high temperatures indicates that cold- and heat stress can be sufficient to trigger
607 programmed cell death (apoptosis).

608 Our results also shed light on the diverse cell-signaling processes that are involved in responding
609 to cold- and heat stress and how these responses may differ between species. The activation by
610 heat stress of key regulatory proteins, for example, phosphorylation on p38-MAPK and JNK,
611 might play important roles in inducing down-stream molecular responses to stress, such as
612 regulating caspase-3 function. Thermal limits to initiation of stress-signaling processes, as
613 discovered in this study, may contribute to establishing whole organism tolerance limits. The
614 temperature ranges over which the cellular stress response can be activated may play important
615 roles in governing the thermal tolerance of the whole organism.

616 Lastly, our data provide additional insights into evolved differences in thermal tolerances between
617 these two congeners of *Mytilus*. Relative to *M. californianus*, *M. galloprovincialis* appears, by

618 several criteria, to be more robust in the face of thermal stress. Thus, the invasive species
619 exhibited a lower amount of single- and double-stranded DNA damage and greater hemocyte
620 membrane stability against cold- and heat stress. In addition, activation of p38-MAPK and JNK
621 was greater in the invasive species than in the native species. Whereas the initiation of a strong
622 stress response might be interpreted as a reflection of a high level of damage to cells, it could
623 alternatively be an indication of a relative high capacity for dealing with such damage. Thus, a
624 capacity to initiate a stronger stress response and to do so rapidly might be a mechanistic basis for
625 greater tolerance in stress-resistant species. Further comparative studies of the downstream
626 consequences of early cell-signaling events are clearly warranted. The physiological differences
627 found in past studies and the present investigation may provide at least a partial explanation for
628 this invasive species' ability to enter and thrive in habitats at numerous sites around the globe.

629

630 **ACKNOWLEDEMENTS**

631 We would like to thank Dr. Xiande Liu (Jimei University) for help with the statistical analysis.

632 This research was funded by National Science Foundation grant IOS-0718734 to GNS and

633 National Science Foundation grant of China 41076076 to CLY.

634

635 **REFERENCES**

636 **Anestis, A., Lazou, A., Pörtner, H.O. and Michaelidis, B.** (2007). Behavioral, metabolic, and
637 molecular stress responses of marine bivalve *Mytilus galloprovincialis* during long-term
638 acclimation at increasing ambient temperature. *Am. J. Physiol. Regul. Integr. Comp. Physiol.*
639 **293**, R911-R921.

640 **Anestis, A., Pörtner, H.O., Lazou, A. and Michaelidis, B.** (2008). Metabolic and molecular
641 stress responses of sublittoral bearded horse mussel *Modiolus barbatus* to warming sea water:
642 implications for vertical zonation. *J. Exp. Biol.* **211**, 2889-2898.

643 **Ashby, J., Tinwell, H., Lefevre, P.A. and Browne, M.A.** (1995). The single cell gel
644 electrophoresis assay for induced DNA damage (comet assay): measurement of tail length and
645 moment. *Mutagenesis.* **10**, 85-90.

646 **Braby, C.E. and Somero, G.N.** (2006a). Ecological gradients and relative abundances of native

647 (*Mytilus trossulus*) and invasive (*Mytilus galloprovincialis*) blue mussels in the California
648 hybrid zone. *Mar. Biol.* **148**, 1249-1262.

649 **Braby, C.E. and Somero G.N.** (2006b). Following the heart: temperature and salinity effects on
650 heart rate in native and invasive species of blue mussels (genus *Mytilus*). *J. Exp. Biol.* **209**,
651 2554-2566.

652 **Brown, L. and Benchimol, S.** (2006). The involvement of MAPK signaling pathways in
653 determining the cellular response to p53 activation: cell cycle arrest of apoptosis. *J. Biol. Chem.*
654 **281**, 3832–3840

655 **Cajaraville, P.M. and Pal, S.G.** (1995). Morphofunctional study of the haemocytes of the bivalve
656 mollusc *Mytilus galloprovincialis* with emphasis on the endolysosomal compartment. *Cell*
657 *Struct. Funct.* **20**, 355-367.

658 **Camus, L., Grøsvik, B.E., Børseth, J.F., Jones, M.B. and Depledge, M.H.** (2000). Stability of
659 lysosomal and cell membranes in haemocytes of the common mussel (*Mytilus edulis*): effect of
660 low temperatures. *Mar. Environ. Res.* **50**, 325-329.

661 **Carballal, M.J., Lopez, M.C., Azevedo, C. and Villalbal, A.** (1997). Hemolymph cell types of
662 the mussel *Mytilus galloprovincialis*. *Dis. Aquat. Org.* **29**, 127-135.

663 **Cheng, T. C.** (1981). Bivalves. In *Invertebrates Blood Cells* (ed. N. A. Ratcliffe and A. F.
664 Rowley), pp. 233-300. London: Academic Press.

665 **Cowan, K.J. and Storey, K.B.** (2003). Mitogen-activated protein kinases: new signaling
666 pathways functioning in cellular responses to environmental stress. *J. Exp. Biol.* **206**,
667 1107-1115.

668 **Craig, N. L., and Roberts, J. W.** (1981) Function of nucleoside triphosphate and polynucleotide
669 in *Escherichia coli* recA protein-directed cleavage of phage lambda repressor. *J. Biol. Chem.*
670 **256**, 8039–8044.

671 **Dimitriadis, V.K., Gougoula, C., Anestis, A., Pörtner, H.O. and Michaelidis, B.** (2012).
672 Monitoring the biochemical and cellular responses of marine bivalves during thermal stress by
673 using biomarkers. *Mar. Environ. Res.* **73**, 70-77.

674 **Earnshaw, W. C., Martins, L. M. and Kaufmann, S. H.** (1999). Mammalian caspases: structure,
675 activation, substrates, and functions during apoptosis. *Annu. Rev. Biochem.* **68**, 383-424.

- 676 **Evans, T.G. and Somero, G.N.** (2010). Phosphorylation events catalyzed by major cell signaling
677 proteins differ in response to thermal and osmotic stress among native (*Mytilus californianus*
678 and *Mytilus trossulus*) and invasive (*Mytilus galloprovincialis*) species of mussels. *Physiol.*
679 *Biochem. Zool.* **83**, 984-996.
- 680 **Fields, P.A., Rudomin, E.L. and Somero, G.N.** (2006). Temperature sensitivities of cytosolic
681 malate dehydrogenases from native and invasive species of marine mussels (genus *Mytilus*):
682 sequence-function linkages and correlations with biogeographic distribution. *J. Exp. Biol.* **209**,
683 656-667.
- 684 **Fields, P.A., Zuzow, M. and Tomanek, L.** (2012). Proteomic responses of blue mussel (*Mytilus*)
685 congeners to temperature acclimation. *J. Exp. Biol.* **215**, 1106-1116.
- 686 **Gaitanaki, C., Kefaloyianni, E., Marmari, A. and Beis, I.** (2004). Various stressors rapidly
687 activate the p38-MAPK signaling pathway in *Mytilus galloprovincialis* (Lam.) *Mol. Cell.*
688 *Biochem.* **260**, 119-127.
- 689 **Gaitanaki, C., Mastri, M., Aggeli, I.K.S. and Beis, I.** (2008). Differential roles of p38-MAPK
690 and JNKs in mediating early protection or apoptosis in the hyperthermic perfused amphibian
691 heart. *J. Exp. Biol.* **211**, 2524-2532.
- 692 **Gaitanaki, C., Pliatska, M., Stathopoulou, K. and Beis, I.** (2007). Cu²⁺ and acute thermal stress
693 induce protective events via the p38-MAPK signalling pathway in the perfused *Rana ridibunda*
694 heart. *J. Exp. Biol.* **210**, 438-446.
- 695 **Geller, J. B.** 1999. Decline of a native mussel masked by sibling species invasion. *Conserv. Biol.*
696 **13**, 661 - 664.
- 697 **Gourgou, E., Aggeli, I.K., Beis, I. and Gaitanaki, C.** (2010). Hyperthermia-induced Hsp70 and
698 MT20 transcriptional upregulation are mediated by p38-MAPK and JNKs in *Mytilus*
699 *galloprovincialis* (Lamarck); a pro-survival response. *J. Exp. Biol.* **213**, 347-357.
- 700 **Hauton, C., Hawkins, L.E. and Hutchinson, S.** (1998). The use of the neutral red retention assay
701 to examine the effects of temperature and salinity on haemocytes of the European flat oyster
702 *Ostrea edulis* (L). *Comp. Biochem. Physiol. B* **119**, 619-623.
- 703 **Hilbish, T., Brannock, P., Jones, K., Smith, A., Bullock, B. and Wethey, D.** (2010). Historical
704 changes in the distributions of invasive and endemic marine invertebrates are contrary to global

705 warming predictions: the effects of decadal climate oscillations. *J. Biogeogr.* **37**, 423-431.

706 **Hochachka, P. W. and Somero, G. N.** (2002). Biochemical Adaptation: Mechanism and Process
707 in Physiological Evolution. Oxford: Oxford University Press. Pp 478.

708 **Jiang, X. and Wang, X.** (2004). Cytochrome c-mediated apoptosis. *Annu. Rev. Biochem.* **73**,
709 87-106.

710 **Jones, S.J., Lima, F.P. and Wethey, D.S.** (2010). Rising environmental temperatures and
711 biogeography: poleward range contraction of the blue mussel *Mytilus edulis* L. in the western
712 Atlantic. *J. Biogeogr.* **37**, 2243-2259.

713 **Jones, S.J., Mieszkowska, N. and Wethey, D.S.** (2009). Linking thermal tolerances and
714 biogeography: *Mytilus edulis* (L.) at its southern limit on the east coast of the United States.
715 *Biol. Bull.* **217**, 73-85.

716 **Kefaloyianni, E., Gourgou, E., Ferle, V., Kotsakis, E., Gaitanaki, C. and Beis, I.** (2005). Acute
717 thermal stress and various heavy metals induce tissue-specific pro- or antiapoptotic events via
718 the p38-MAPK signal transduction pathway in *Mytilus galloprovincialis* (Lam.), *J. Exp. Biol.*
719 **208**, 4427-4436.

720 **Klobučar, G. I.V., Štambuk, A., Hylland, K. and Pavlica, M.** (2008). Detection of DNA
721 damage in haemocytes of *Mytilus galloprovincialis* in the coastal ecosystems of Kaštela and
722 Trogir bays, Croatia. *Sci. Total Environ.* **405**, 330-337.

723 **Końca, K., Lankoff, A., Banasik, A., Lisowska, H., Kuszewski, T., Gózdź, S., Koza, Z. and**
724 **Wojcik, A.** (2003). A cross-platform public domain PC image-analysis program for the comet
725 assay. *Mutat. Res.* **534**, 15-20.

726 **Kültz, D.** (2005). Molecular and evolutionary basis of the cellular stress response. *Annu. Rev.*
727 *Physiol.* **67**, 225-257.

728 **Lakhani, S.A., Masud, A., Kuida, K., Porter, G.A. Jr, Booth, C.J., Mehal, W.Z., Inayat, I. and**
729 **Flavell, R.A.** (2006). Caspases 3 and 7: key mediators of mitochondrial events of apoptosis.
730 *Science* **311**, 847-51.

731 **Li, H., Toubiana, M., Monfort, P. and Roch, P.** (2009). Influence of temperature, salinity and *E.*
732 *coli* tissue content on immune gene expression in mussels: Results from a 2005–2008 survey.
733 *Dev. Comp. Immunol.* **33**, 974–979.

- 734 **Li, J. J. and Deshaies, R. J.** (1993). Exercising self-restraint: discouraging illicit acts of S and M
735 in eukaryotes *Cell* **74**, 223–226.
- 736 **Lockwood, B. L., Sanders, J. G. and Somero, G. N.** (2010). Transcriptomic responses to heat
737 stress in invasive and native blue mussels (genus *Mytilus*): molecular correlates of invasive
738 success. *J. Exp. Biol.* **213**, 3548-3558.
- 739 **Lockwood, B.L. and Somero, G.N.** (2011). Invasive and native blue mussels (genus *Mytilus*) on
740 the California coast; the role of physiology in a biological invasion. *J. Exp. Mar. Biol. Ecol.* **400**,
741 167-174.
- 742 **Lowe, D. M. and Pipe, R. K.** (1994). Contaminant induced lysosomal membrane damage in
743 marine mussel digestive cells: An *in vitro* study. *Aquat. Toxicol.* **30**, 357–365.
- 744 **Lowe, D. M., Fossato, V. U. and Depledge, M. H.** (1995). Contaminant induced lysosomal
745 membrane damage in blood cells of mussels *M. galloprovincialis* from the Venice Lagoon: An
746 *in vitro* study. *Mar. Ecol. Prog. Ser.* **129**, 189–196.
- 747 **Micic, M., Bihari, N., Jaksic, Z., Muller, W. E.G. and Batel, R.** (2002). DNA damage and
748 apoptosis in the mussel *Mytilus galloprovincialis*. *Mar. Environ. Res.* **53**, 243–262.
- 749 **Murai, H., Hiragami, F., Kawamura, K., Motoda, H., Koike, Y., Inoue, S., Kumagishi, K.,**
750 **Ohtsuka, A. and Kano, Y.** (2010). Differential response of heat-shock-induced p38 MAPK and
751 JNK activity in PC12 mutant and PC12 parental cells for differentiation and apoptosis. *Acta.*
752 *Med. Okayama* **64**, 55-62.
- 753 **Nitiss, J. L.** (1998). Investigating the biological functions of DNA topoisomerases in eukaryotic
754 cells. *Biochim. Biophys. Acta* **1400**: 63-68.
- 755 **Ori, Y., Herman, M., Weinstein, T., Chagnac, A., Zevin, D., Milo, G., Gafter, U. and Malachi,**
756 **T.** (2005). Spontaneous DNA repair in human peripheral blood mononuclear cells. *Biochem.*
757 *Biophys. Res. Commun.* **320**, 578–586.
- 758 **Parolini, M., Quinn, B., Binelli, A. and Provini, A.** (2011). Cytotoxicity assessment of four
759 pharmaceutical compounds on the zebra mussel (*Dreissena polymorpha*) haemocytes, gill and
760 digestive gland primary cell cultures. *Chemosphere.* **84**, 91-100.
- 761 **Prasad, R., Beard, W. A., Batra, V. K., Liu, Y., Shock, D. D. and Wilson, S. H.** (2011). A review
762 of recent experiments on step-to-step “hand-off” of the DNA intermediates in mammalian base

763 excision repair pathways. *Mol. Biol. (Mosk)*. **45**, 586–600.

764 **Roberts, K.P., Sobrino, J.A., Payton, J., Mason, L.B. and Turesky, R.J.** (2006). Determination
765 of apurinic/aprimidinic lesions in DNA with high-performance liquid chromatography and
766 tandem mass spectrometry. *Chem. Res. Toxicol.* **19**, 300–309.

767 **Schneider, K.R.** (2008). Heat stress in the intertidal: comparing survival and growth of an
768 invasive and native mussel under a variety of thermal conditions. *Biol Bull.* **215**, 253-64.

769 **Singh, N.P., McCoy, M.T., Tice, R. and Schneider, E.L.** (1988). A simple technique for the
770 quantitation of low levels of DNA damage in individual cells. *Exp. Cell Res.* **175**, 184-191.

771 SPSS[®] Base 13.0 User'S Guide, (2004). SPSS Inc. 409-424.

772 **Tomanek, L. and Zuzow, M.J.** (2010). The proteomic response of the mussel congeners *Mytilus*
773 *galloprovincialis* and *M. trossulus* to acute heat stress: implications for thermal tolerance limits
774 and metabolic costs of thermal stress. *J. Exp. Biol.* **213**, 3559-3574.

775 **Wallace, S. S.** (1994). DNA damages processed by base excision repair—biological consequences.
776 *Int. J. Radiat. Biol.* **66**, 579–589.

777 **Wepener, V., Bervoets, L., Mubiana, V. and Blust, R.** (2008). Metal exposure and biological
778 responses in resident and transplanted blue mussels (*Mytilus edulis*) from the Scheldt estuary.
779 *Mar. Pollut. Bull.* **57**, 624 - 631.

780 **Yao, C.L., Wu, C.G., Xiang, J.H., Li, F.H., Wang, Z.Y. and Han, X.Z.** (2008). The lysosome
781 and lysozyme response in Chinese shrimp *Fenneropenaeus chinensis* to *Vibrio anguillarum* and
782 laminarin stimulation. *J. Exp. Mar. Biol. Ecol.* **363**, 124-129.

783 **Figure legends.**

784 Fig. 1. Measurements of DNA damage in hemocytes of mussels following temperature
785 stress. Cell: a mussel hemocyte after single-cell gel electrophoresis; Head: head diameter; Tail: tail
786 length; Stain: SYBR green.

787
788 Fig. 2. Single-stranded DNA breakage in hemocytes of mussels after acute cold- and heat
789 stress. A. *M. californianus*, B. *M. galloprovincialis* (13°C = control). Statistical significance was
790 determined by two-way ANOVA with temperature and stress time as factors. Asterisks denote
791 statistically significant differences ($p < 0.05$) between experimental treatments (high- and low
792 temperature stress for varying times) and the control (13°C specimens).

793
794 Fig. 3. Double-stranded DNA breakage in hemocytes of mussels after heat and cold stress
795 (13°C = control). A. *M. californianus* B. *M. galloprovincialis*. Statistical significance was
796 determined by two-way ANOVA with temperature and stress time as factors. Asterisks denote
797 statistically significant differences ($p < 0.05$) between experimental treatments (high- and low
798 temperature stress for varying times) and the control (13°C specimens).

799
800 Fig. 4. Analysis of phosphorylation on p38 (Thr180/Tyr182) and phosphorylation on
801 JNK/SAPK (Thr-183/ Tyr-185) in hemocytes of *M. californianus* and *M. galloprovincialis* after
802 low- and high-temperature stress (13°C = control). A. phospho-p38 (Thr-180/Tyr-182) in *M.*
803 *californianus*; B. phospho-p38 (Thr-180/Tyr-182) in *M. galloprovincialis*; C.
804 phospho-JNK1/SAPK (Thr-183/ Tyr-185, p46 band) in *M. californianus*; D.
805 phospho-JNK1/SAPK (Thr-183/ Tyr-185, p46 band) in *M. galloprovincialis*; E. phospho-JNK2/3
806 (Thr-183/ Tyr-185, p46 band) in *M. californianus*; F. phospho-JNK2/3 (Thr-183/ Tyr-185, p46
807 band) in *M. galloprovincialis*; Statistical significance was determined by two-way ANOVA with
808 temperature and stress time as factors. Asterisks denote statistically significant differences
809 ($p < 0.05$) between experimental treatments (high- and low temperature stress for varying times)
810 and the control (13°C specimens).

811

812 Fig. 5. Analysis of pro- and active caspase-3 expression in hemocytes of *M. californianus*
813 and *M. galloprovincialis* after acute cold- and heat stress. A. expression of pro-caspase-3 in *M.*
814 *californianus*; B. expression of pro-caspase-3 in *M. galloprovincialis*; C. expression of active
815 caspase-3 in *M. californianus*; D. expression of active caspase-3 in *M. galloprovincialis*.
816 Statistical significance was determined by two-way ANOVA with temperature and stress time as
817 factors. Asterisks denote statistically significant differences ($p<0.05$) between experimental
818 treatments (high- and low temperature stress for varying times) and the control (13°C specimens).

819

820 Fig. 6. Numbers of non-viable hemocytes after acute cold- and heat stress. *M.*
821 *californianus* (A) and *M. galloprovincialis* (B). Statistical significance was determined by
822 two-way ANOVA with temperature and stress time as factors. Asterisks denote statistically
823 significant differences ($p<0.05$) between experimental treatments (high- and low temperature
824 stress for varying times) and the control (13°C specimens).

825

826 Fig. 7. Mean NRR times in hemocyte lysosomes of *M. californianus* (A) and *M.*
827 *galloprovincialis* (B) at different time intervals of exposure to acute cold- and heat stress.
828 Statistical significance was determined by two-way ANOVA with temperature and stress time as
829 factors. Asterisks denote statistically significant differences ($p<0.05$) between experimental
830 treatments (high- and low temperature stress for varying times) and the control (13°C specimens).

831

832

833

834

835

836

837

838

839

840

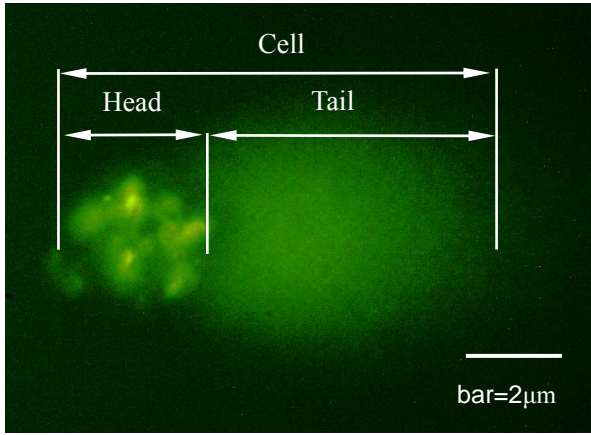
841

842

843

844

845



846

847 Fig. 1.

848

849

850

851

852

853

854

855

856

857

858

859

860

861

862

863

864

865

866

867

868

869

870

871

872

873

874

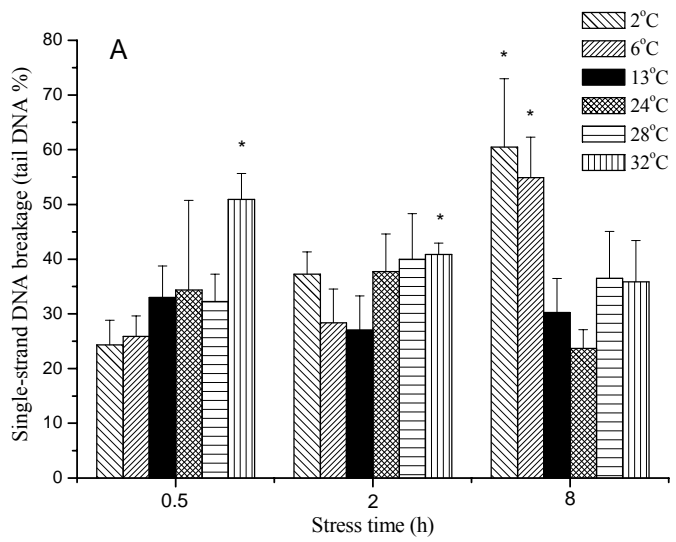
875

876

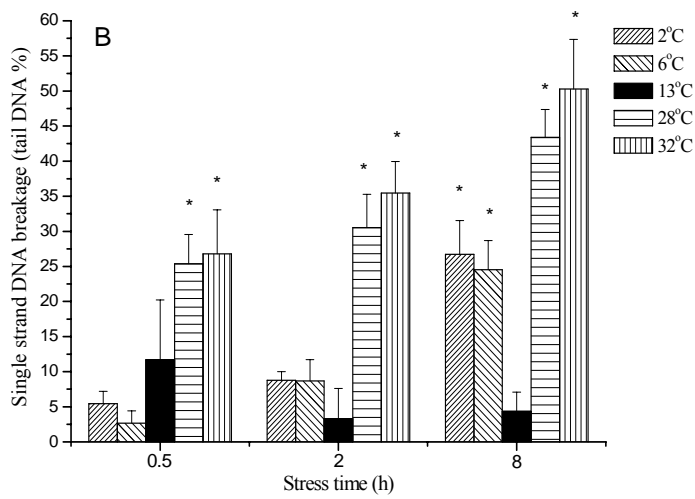
877

878

879



880



881

882 Fig. 2.

883

884

885

886

887

888

889

890

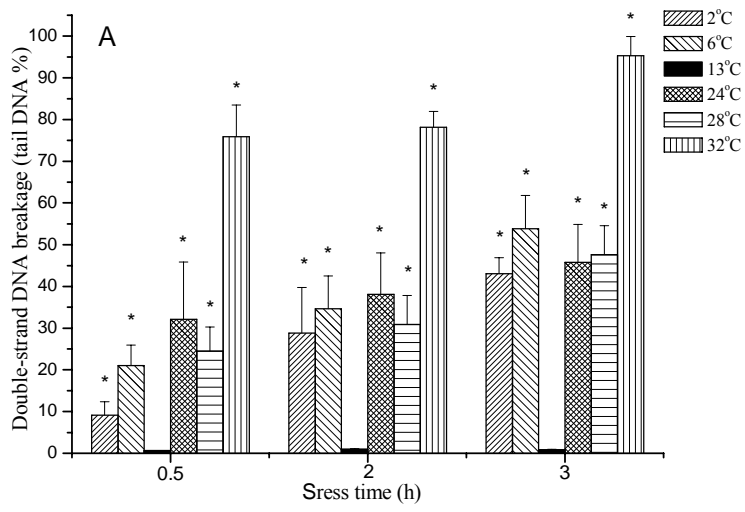
891

892

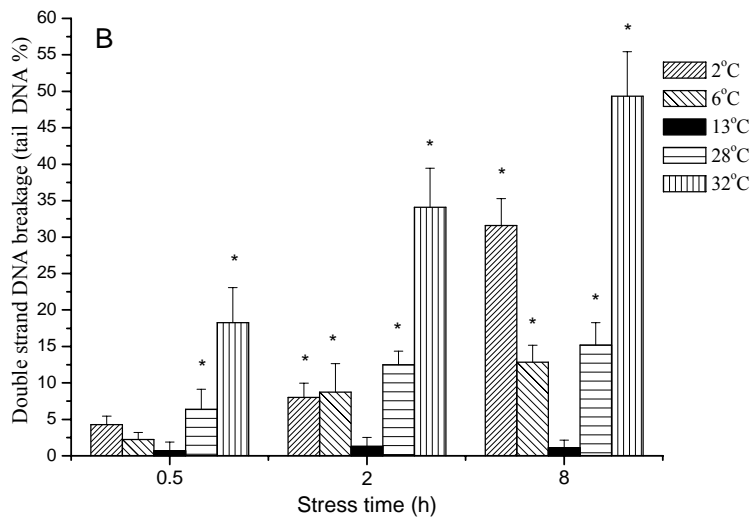
893

894

895



896



897

898 Fig. 3.

899

900

901

902

903

904

905

906

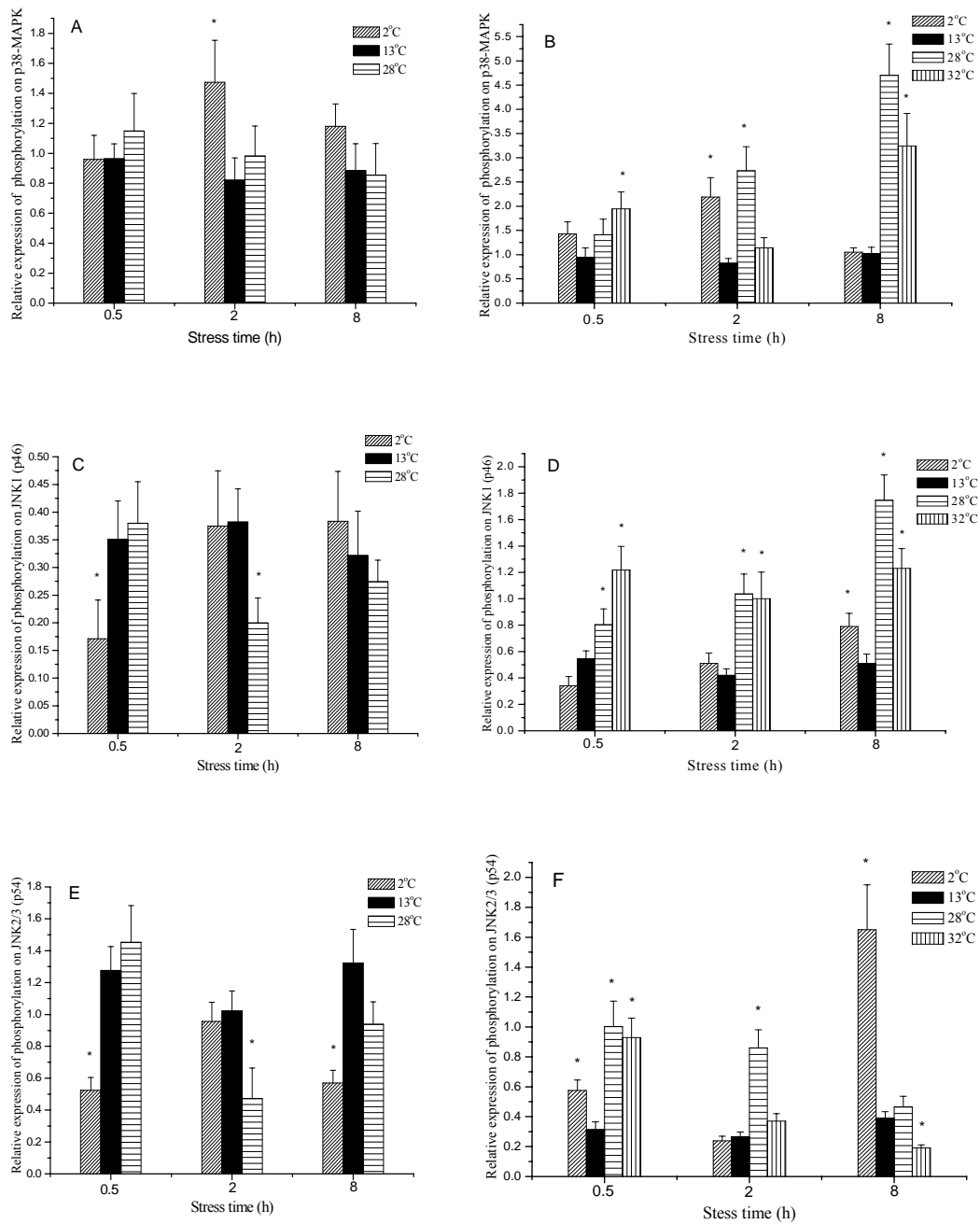
907

908

909

910

911



912

913

914

915

916

917 Fig. 4.

918

919

920

921

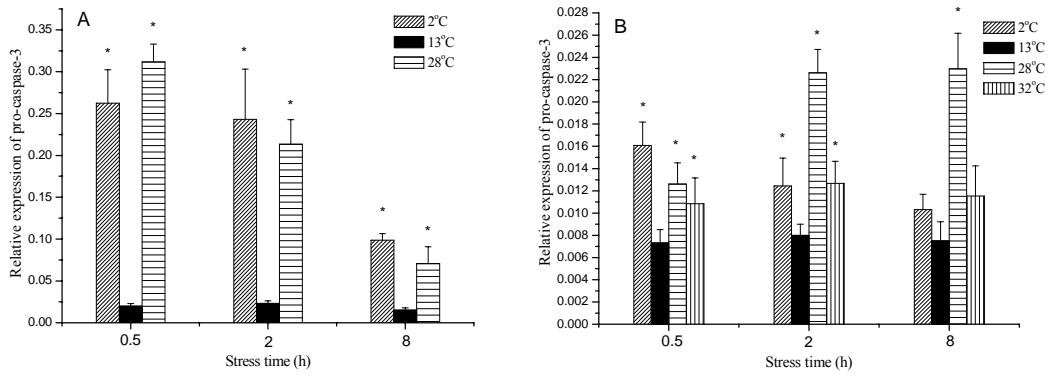
922

923

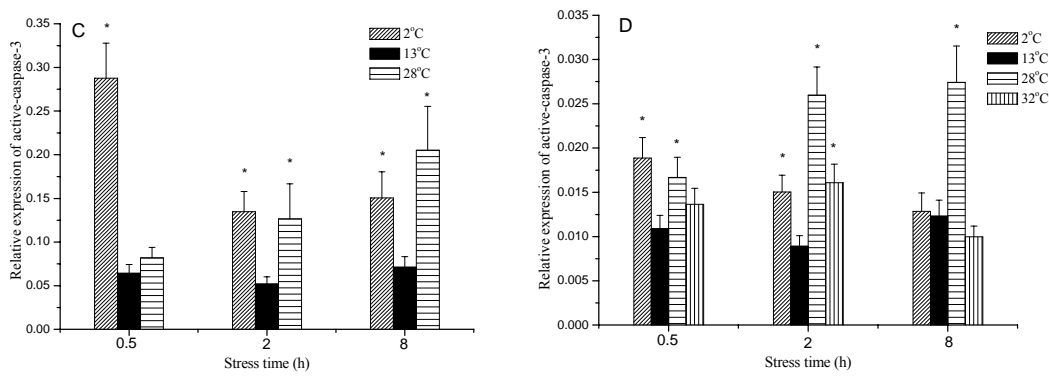
924

925

926



927



928

929

Fig. 5.

930

931

932

933

934

935

936

937

938

939

940

941

942

943

944

945

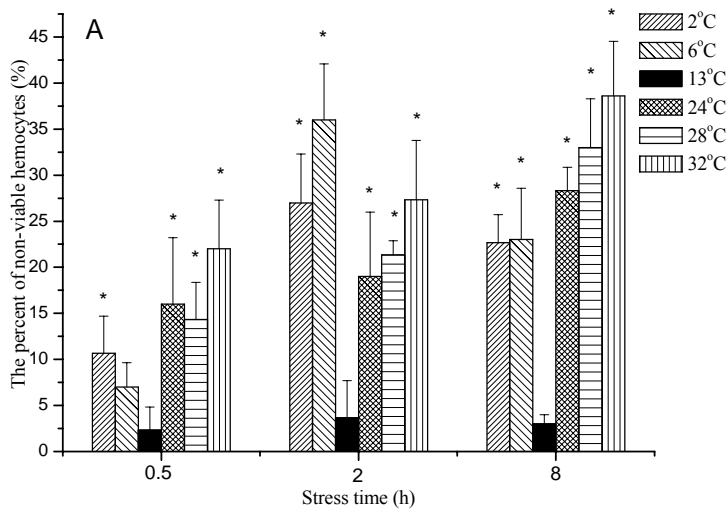
946

947

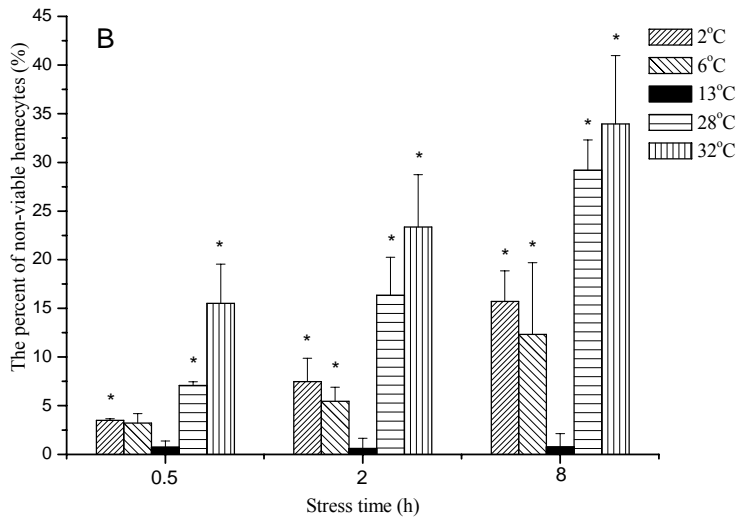
948

949

950



951



952

953

Fig. 6.

954

955

956

957

958

959

960

961

962

963

964

965

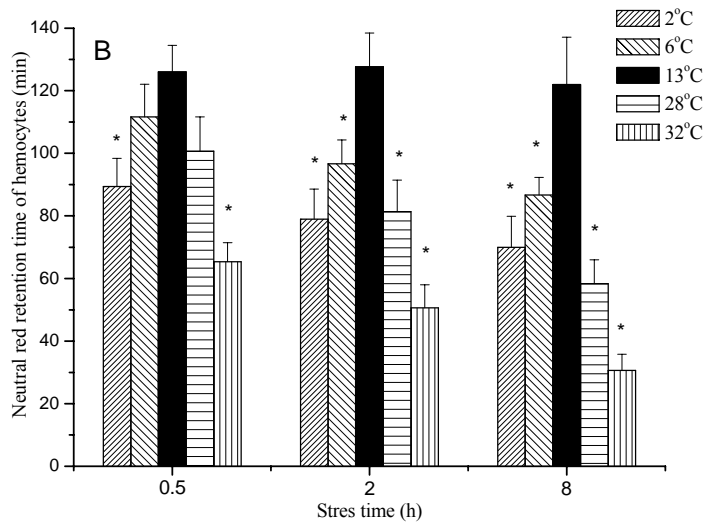
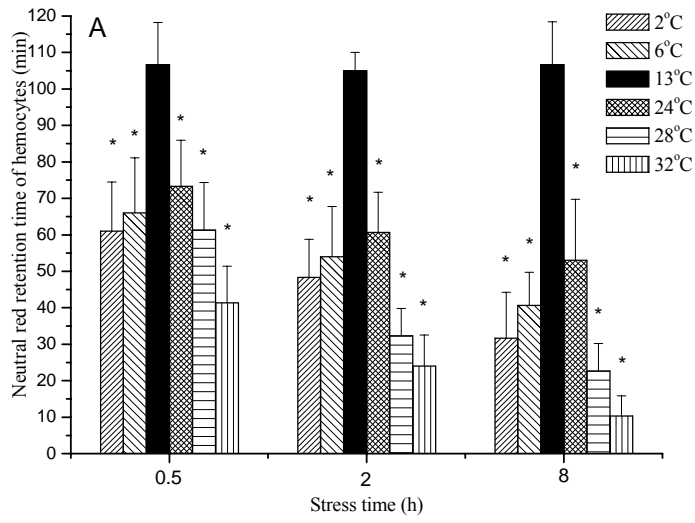


Fig. 7.

